

Deciphering optimal mixed-mode ventilation in the tropics using reinforcement learning with explainable artificial intelligence

Xilei Dai^a, Siyu Cheng^a and Adrian Chong^{a,*}

^aDepartment of the Built Environment, College of Design and Engineering, National University of Singapore, 4 Architecture Drive, Singapore, 117566, Singapore

ARTICLE INFO

Keywords:

Mixed-mode ventilation
Reinforcement learning
Explainable artificial intelligence
Shapley additive explanations
Window opening
Cooling setpoint

ABSTRACT

The application of mixed-mode ventilation (MMV) in the tropics is challenging, given its hot and humid climate. Consequently, there are limited periods when operating in natural ventilation (NV) is desirable. Furthermore, the potential to use NV diminishes at locations characterized by generally light winds. Given the complex interactions in MMV, this study aims to use reinforcement learning (RL) to identify relationships that can further reduce cooling energy use while maintaining occupant thermal comfort. The control variable variables considered include the percentage of window opening area and dynamic cooling setpoint temperature. Results show that RL can achieve a 52% reduction in cooling energy while maintaining good thermal comfort and indoor air quality compared to the existing baselines that typically involve switching between NV and air-conditioning based on outdoor conditions. We then developed an Explainable AI (XAI) framework to prompt building scientists toward new insights into MMV control in the tropics, which consists of shapley additive explanations (SHAP) and decision tree. The SHAP is able to improve the transparency of RL strategy by revealing the impact of each input on the final decision and the decision tree can extract the key control rules from RL. Using the XAI framework, this study also identified that the RL algorithm was taking advantage of the internal thermal mass to increase cooling efficiency. The extracted rules are further applied to the actual testbed, showing the feasibility of the rules extracted by XAI approach.

1. Introduction

The building and construction sector is responsible for a large part of final energy use (36%) and energy-related CO₂ emissions (39%) [1]. Therefore, it is necessary to focus on energy saving in the building sector via advanced technologies while ensuring liveability and eco-friendliness. One widely-recognized strategy to reduce HVAC energy consumption is to combine natural ventilation (NV) from operable windows with active cooling systems, also referred to as mixed-mode ventilation (MMV) [2, 3]. MMV has also been shown to offer higher occupant satisfaction and improved indoor air quality by providing occupants with higher degrees of control over their indoor environment [4].

The energy-saving potential of MMV has been previously investigated. Salcido et al. [4] reviewed MMV systems in office buildings. They found that 40% of HVAC energy can be saved by optimizing window operation schedules and up to 75% by alternating between natural and AC. Ezzeldin and Rees [5] studied the energy-saving potential of MMV in arid climates and concluded that adopting an MMV strategy can significantly reduce cooling plant energy by more than 40%. Wang and Chen [6] simulated the energy consumption for several MMV office buildings across America using EnergyPlus. They investigated the energy saving of MMV in five climate zones, including very hot and humid, very hot and dry, hot and dry, marine, and warm and humid. The saving rate varies among climate zones, ranging from

*Corresponding author

 adrian.chong@nus.edu.sg (A. Chong)

ORCID(s): 0000-0003-0903-5341 (X. Dai); 0000-0002-4133-5507 (S. Cheng); 0000-0002-9486-4728 (A. Chong)

6–91% with MMV. [7] conducted a dynamic simulation for a typical office building in the dry-summer subtropical zone under the mixed-mode operation. They concluded that using a mixed-mode system can save annual energy by 31%. The climate impacts the energy-saving performance of MMV significantly. However, there are limited studies investigating the feasibility of MMV in the tropics. Additionally, locations with a year-round hot and humid climate have been shown to have little to no potential for NV [8] and thus MMV. To alleviate the lack of natural ventilation and provide occupant thermal comfort, ceiling and desk fans are often used to increase air movement within a space [9, 10]. More recently, studies have also taken advantage of the elevated air movement from desk and ceiling fans to increase space cooling setpoint temperature leading to reductions in HVAC energy consumption [11, 12]. Consequently, using elevated air movement (such as with ceiling fans) to supplement MMV provides an opportunity to enable MMV in the tropics [13].

Broadly speaking, MMV can be classified into three control schemes: change-over, concurrent, and zoned [14]. For MMV control, optimizing the window opening strategy is essential to maximize energy saving because it takes advantage of NV by opening windows to significantly reduce cooling energy [4]. The most conventional strategy is the rule-based control strategy. Breesch et al. [15] developed a rule-based strategy for nighttime window operation strategy with consideration of several factors, including indoor/outdoor temperature, outdoor wind speed, etc. This rule-based strategy helps to cool down the indoor air and decrease the peak indoor air temperature. Eftekhari and Marjanovic [16] designed a rule-based controller that considers outside wind velocity, direction, outside and inside temperatures as inputs to decide the window opening area. By applying the controller in the decision of window operation, the indoor thermal comfort for a test room improved significantly. Wang and Greenberg [17] set the window to open when the outdoor air temperature is lower than the upper bound of the adaptive thermal comfort zone, reducing HVAC energy by 18.3–46.8% in summer for buildings located in humid continental, humid subtropical, and Mediterranean mild climates. Similarly, Fiorentini et al. [18] used the adaptive thermal comfort model as the guideline to select ventilation mode for buildings located in the warm temperate climate zone of Australia. This rule-based strategy was tested in an MMV house. The result showed that nearly 70% reduced the daily cooling energy consumption with a satisfactory indoor thermal environment in summer.

Although straightforward and easy to implement, the prescriptive rule-based control strategy is sub-optimal. This is because predictive information is not taken into consideration for the decision of window operation. A more advanced control strategy is model predictive control (MPC), which optimizes the decision variables by simulating the buildings over a finite time horizon [19, 20, 21]. Previous studies also investigated the MPC strategy to increase energy saving for MMV buildings. By integrating the EnergyPlus model into the optimization framework, May-Ostendorp et al. [22] used the particle swarm optimization (PSO) algorithm to calculate the optimal window status (closed or full opening) over a 24-h planning horizon for an office building. Hu and Karava [23] also developed a framework that used a

thermal network to predict building thermal dynamics and used the PSO algorithm to decide the optimal window status (open/close) for a mixed-mode test office. Similarly, this framework was also used for whole-building window control and got significant energy-saving [24]. Besides heuristic algorithms, optimization programming was also used to calculate the optimal window operation. In [25], the day was divided into four periods, which were early evening, transition period, and two nighttime periods. The integer programming was utilized to find the optimal control mode from four predefined ventilation modes for each period. Although the algorithms mentioned above can be used to determine window operation to save cooling energy, both heuristic algorithm and optimization programming are time-consuming since they need to conduct the optimization algorithm at every control time step. This makes it challenging to apply them for the real-time decision of window-opening. In another aspect, the performance of MPC relies on the information predicted by the model. Given that the control environment is impacted by unexpected disturbances, the prediction model may become biased. Due to this, the performance of MPC may be negatively impacted.

Recently, many studies used reinforcement learning (RL) or deep learning algorithms to optimize cooling systems and achieved significant benefits by optimizing HVAC system control [26, 27, 28, 29]. It is reasonable to infer that RL is also an algorithm to optimize the control for MMV buildings. Moreover, the calculation time for such data-driven algorithms is short after they are trained [30], making it possible to apply them in real-time control for window opening. Chen et al. [31] recently optimized the window status (open/close) schedule using RL and achieved the energy saving of 13% and 23% for MMV buildings in hot-and-humid Miami and warm-and-mild Los Angeles, respectively. However, only binary window opening (open/close) was considered in their study. Higher energy-saving performance can be achieved by considering the window opening area and cooling setpoint. Furthermore, both Luo et al. [32] and Kim et al. [33] concluded that the adaptive comfort model was applicable to MMV buildings. The energy-saving potential of the RL control strategy with the constraint of adaptive comfort is yet to be investigated.

In another aspect, although the RL algorithms are able to increase the energy-saving potential for mixed-mode buildings, such artificial intelligence (AI) algorithms are difficult to explain, which leads to maintainability problems for real application in building management systems [34]. Explainable artificial intelligence (XAI) was proposed to 1) produce more explainable models while maintaining high performance and 2) enable humans to understand and appropriately trust the AI model [35]. The common approaches include feature attribution [36, 37], attention-based network [38] and self-explaining mechanism [39]. Among these, the attention-based network and the self-explaining mechanism improve the interpretation of the AI model by adding additional layers/modules to the models. By doing this, the models can provide visual explanations. The feature attribution aims to explain the AI model by revealing the relationship between input and output in an explainable way. Previous studies have applied this approach to explain the model for robot control [40], image classification [41]. It can be seen that these XAI approaches may be useful to explain the reasons for a model's prediction and consequently provide insights into the model's decision-making

Table 1

Comparison of the characteristic of rule-based control, MPC, RL control and XAI-rule control

	Rule-based	MPC	RL control	XAI-rule
Strength	1. Interpretable 2. Implementable 3. Maintainable	1. Based on prediction model 2. Interpretable 3. Median to high performance	1. High performance	1. Interpretable 2. Implementable 3. Maintainable 4. Near high-performance
Disadvantage	1. Low performance	1. Lack of scalability 2. Lack of maintainability	1. Lack of interpretability 2. Lack of scalability 3. Lack of maintainability 4. Need efforts to train	1. Need efforts to train

process. In the field of MMV control, although the previous study has developed an RL algorithm to optimize the MMV control [31], little study has applied XAI to explain the control principle of RL for MMV. Therefore, it is worth applying the XAI for MMV control optimization. By doing this, the reliability of the RL for MMV can be further confirmed. Moreover, it is likely to learn the new control insights for MMV control from XAI, which might be able to transfer to other buildings directly. The comparison of the characteristic of rule-based control, RL control, and XAI-rule control are summarized in Table 1.

The purpose of this study is to critically examine the relationships that can further reduce cooling energy use while maintaining occupant thermal comfort using RL. The objectives of this study are to: 1) investigate the strength of RL strategy in MMV building control by using the window-opening area and the cooling setpoint as the control variables for MMV; 2) develop an XAI framework to improve the transparency and engender user trust for the RL strategy; 3) bridge the gap between building science and the application of RL using XAI approaches, prompting new insights that can be used to generate easily implementable rules for optimal MMV operation.

2. Methods

The methodology of this study consists of two parts. First, we investigate the application of RL for the optimal control of mixed-mode ventilated buildings. Second, we used the XAI framework to provide insights into the RL strategy and extract rulesets from the optimal RL control strategy. We use a virtual testbed to compare and evaluate the performance of the RL control strategy and the rulesets extracted using XAI.

2.1. Baselines and RL control strategy

Table 2 lists the control variables and constraints considered in our application of RL for MMV. The constraints for the strategies are implemented as the reward functions in RL. In RL-1, we investigate the energy-saving potential of dynamically varying window opening size (0–100% window opening area in 25% stepsize). In RL-2, we extended RL-1 with dynamic cooling setpoint temperature (24–27°C in 1°C stepsize) as an additional control variable. Lastly,

Table 2

List of control variables and constraints of the three RL strategies investigated in this study.

RL strategy	Ventilation mode	Control variables		Constraints
		Window-opening area (%)	cooling setpoint (°C)	
RL-1	Change-over	[0, 25, 50, 75, 100]	24	Energy, Adaptive thermal comfort
RL-2	Change-over	[0, 25, 50, 75, 100]	[24, 25, 26, 27]	Energy, Adaptive thermal comfort
RL-3	Change-over	[0, 25, 50, 75, 100]	[24, 25, 26, 27]	Energy, Adaptive thermal comfort& IAQ

in RL-3, we extended RL-2 by adding other constraints to maintain good indoor air quality in the occupied space. To benchmark the proposed RL control strategies, we also compare their performance to two baseline strategies that switch between a fully closed and fully opened window based on the outdoor temperature. Specifically, as shown in Eq. 1, the window is fully open when the outdoor temperature, T , is lower than the threshold T_b . Otherwise, it is closed when the outdoor temperature is higher than the threshold T_b . We select 29°C and 30°C as the thresholds for the baseline strategy, which are named baseline-29 and baseline-30, respectively. The baseline-29 means the window is fully open when the outdoor temperature is lower than 29°C, while it is fully closed when the outdoor temperature is higher than 29°C; the baseline-30 means the window is fully open when the outdoor temperature is lower than 30°C, while it is fully closed when the outdoor temperature is higher than 30°C.

$$\text{Window opening area} = \begin{cases} 100\%, & T \leq T_b \\ 0\%, & T > T_b \end{cases} \quad (1)$$

2.2. Deep Q-learning

Deep Q-learning is used for the RL control in this study. Deep Q-learning is a model-free RL algorithm that learns the values of a few actions in a particular state. It uses a fully connected network as the control agent. A significant advantage of deep Q-learning is learning the nonlinear relationship between inputs and predicted rewards, making it a suitable algorithm for optimizing control for MMV.

Figure 1 shows the workflow of the deep Q-learning. Given the state S_t at time step t , the agent estimates the Q value of alternative actions, and the action with the highest Q value is selected and applied to the environment. After that, the environment updates the state S_{t+1} at the next time step $t + 1$ and repeats the above process. In this study, the environment is the virtual testbed office, which is described in Section 2.4. The states are indoor temperature, outdoor temperature, outdoor relative humidity and solar radiation, which are common inputs for decision of mixed-mode ventilation [42]. We selected these variables because these are potential variables that impact cooling energy.

The agent is a fully-connected artificial neural network in this study. After receiving the state S_t at time t , the agent estimates the value of each available action. In this MMV control problem, we investigated the performance of MMV

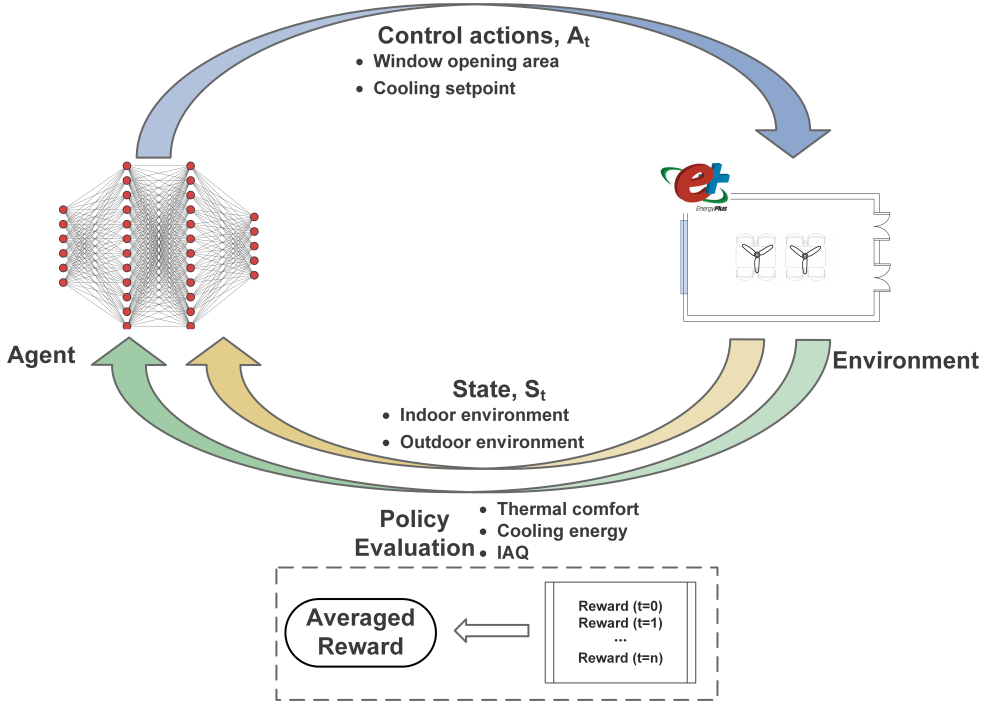


Figure 1: Deep Q-learning for MMV building control of window opening area and cooling setpoint. At each time step, the agent takes the state as inputs and predicts the optimal action for next time step.

under two different settings. One setting is that only window opening is the control variable and the possible window opening areas are 0%, 25%, 50%, 75% and 100%. The cooling setpoint is always 24°C when the window is closed. Another setting is that the control variables are both the window opening area and the cooling setpoint. Under this setting, the cooling setpoint can be 24°C - 27°C with an interval of 1°C when the window is closed. Therefore, under the first setting which only controls the window opening area, the set of actions contains five possible actions; under the second setting, which controls both the window opening area and the cooling setpoint, it includes eight possible actions.

During the training of the agent, the Q value under the current time step is estimated as follows.

$$Q^*(s_t, a_t) = r_t + \gamma Q(s_{t+1}, \text{argmax}_{a'} Q'(s_t, a_t)) \quad (2)$$

where $Q^*(s_t, a_t)$ is the expected Q value when taking the action a_t at state s_t ; r_t is the actual reward at time step t ; $Q(s_{t+1}, \text{argmax}_{a'} Q'(s_t, a_t))$ is the expected Q value at next time step when taking the action a_t that lead to the maximal Q value at time step t ; and γ is the discount factor for the estimation of future Q value.

The training target is to minimize the error between Q^* and Q . So the smooth L1 loss function during the training process is defined as follows [43]:

$$l_n = \begin{cases} 0.5(Q^* - Q)^2 / \beta, & \text{if } |Q^* - Q| < \beta \\ |Q^* - Q| - 0.5 * \beta, & \text{otherwise} \end{cases} \quad (3)$$

To guide the training of the RL agent, the reward function defines an objective function to be maximized in the RL problem. The maximization procedure is conducted based on the interaction between the RL agent and the environment, as shown in Figure 1. To take the cooling energy, thermal comfort and IAQ into consideration, the instant reward, r_t , is calculated using Eq. 4-7.

$$r_t = w_1 \times r_{\text{energy}} + w_2 \times r_{\text{tem}} + w_3 \times r_{\text{IAQ}} \quad (4)$$

$$r_{\text{energy}} = \frac{E_1^2 - E_t^2}{E_1^2} \quad (5)$$

$$r_{\text{tem}} = \begin{cases} \exp\left(\frac{(T_t - T_1)^2}{2 \times T_{\text{std}}^2}\right), & \text{if } T_t < 29^\circ\text{C} \\ r_p, & \text{otherwise} \end{cases} \quad (6)$$

$$r_{\text{IAQ}} = \begin{cases} 1, & \text{if } CO_2 < 1000 \text{ ppm} \\ r_p, & \text{otherwise} \end{cases} \quad (7)$$

where r_{energy} , r_{tem} and r_{IAQ} represent the instant reward for cooling energy, thermal comfort and IAQ, respectively. The w_1 , w_2 and w_3 are weighted factors for each instant reward, which are 0.5, 3.5 and 1, respectively. For r_{energy} , E_t is the instant cooling rate at time t and E_1 is the constant of cooling rate, which is set as 3000W. For r_{tem} , T_t is the indoor air temperature at time t . T_1 and T_{std} are the constants of temperature, which are set as 28.5°C and 0.5°C , respectively. r_p is the penalty reward, which is set as -5.

During the training, the performance of the RL is evaluated by the annual cooling energy consumption and the corresponding indoor thermal comfort of the virtual testbed office. We selected the most energy-efficient strategy for RL-1, RL-2, and RL-3 that meets the requirement of at least 80% of time satisfying the adaptive thermal comfort requirement during NV operation as the control model. The settings of the hyperparameters are listed in Table 3. The training is based on the simulation in June using EnergyPlus and the test is based on the simulation for the whole year.

Table 3

The setting of the hyperparameters for training the RL algorithm

Hyperparameters	Values
Hidden layers	2
Nodes for hidden layers	64-64
ϵ -greedy rate	0.01
Learning rate	10^{-4}
Batch size	128
Optimization method	SGD

2.3. XAI framework for knowledge extraction

Since deep Q-learning is a black-box model that can be difficult to explain and interpret, we applied XAI to extract the knowledge from the RL algorithm to make it understandable to humans. The first step of the XAI framework is to reveal the importance of each input parameter for a particular prediction. By doing this, we can understand which parameters play an important role for RL and how the decision of RL is made in different environments. This information can strengthen user trust, and prompt understanding of the process being modeled. In this study, we apply Kernel SHAP (SHapley Additive exPlanations) to interpret the relationship between inputs and the corresponding actions [36], which is a combination of linear local interpretable model-agnostic explanations (LIME) and classic Shapley value estimation. The Kernel SHAP can reveal the local importance of features, and show how the feature values impact the final output by calculating the Shapley value. The Kernel SHAP is implemented using the SHAP package [44]. The Shapley value, ϕ , can be calculated as follows:

$$\phi_i(f, x) = \sum_{z' \subseteq x'} \frac{|z'|!(M - |z'| - 1)!}{M!} [f_x(z') - f_x(0)] \quad (8)$$

where $z' \in \{0, 1\}^M$, M is the number of the simplified input features. $|z'|$ is the number of non-zero entries in z' , and $z' \subseteq x'$ means all z' vectors where the non-zero entries are a subset of the non-zero entries in x' .

LIME uses the local linear explanation model, g as shown in Equation 9 to locally approximate the model f around a given prediction. Explanation model usually use simplified inputs x' to map the original inputs through a mapping function $x = h_x(x')$. Local methods try to make $g(z') \approx f(h_x(z'))$ when $z' \approx x'$.

$$g(z') = \phi_0 + \sum_{i=1}^M \phi_i z'_i \quad (9)$$

where $\phi_i \in R$. To find ϕ , LIME minimizes objective function as below:

$$\xi = \underset{g \in G}{\operatorname{argmin}} L(f, g, \pi_{x'}) + \Omega(g) \quad (10)$$

where L is the square loss function over samples in the simplified input space weighted by local kernel $\pi_{x'}$. Ω is the function to penalize the complexity of g .

In Kernel SHAP, the specific forms of π'_x , L , and Ω are described in Equation 11-13:

$$\Omega(g) = 0 \quad (11)$$

$$\pi_{x'}(z') = \frac{(M - 1)}{(M \text{ choose } |z'|)|z'|(M - |z'|)} \quad (12)$$

$$L(f, g, \pi_{x'}) = \sum_{z' \in Z} [f(h_x(z')) - g(z')]^2 \pi_{x'}(z') \quad (13)$$

To further understand the control logic of RL, we apply an interpretable surrogate model to learn the predictions of the original black-box model in order to interpret the latter [45]. In this study, we used a decision tree as the surrogate model because it is easy to understand for humans. With the extracted knowledge, we can further confirm the reliability of the strategy by combining the extracted knowledge and building science knowledge.

After getting the optimal control schedule of the window opening area and cooling setpoint from the RL algorithm, the decision tree is applied to learn the window opening area and the cooling setpoint schedule. The inputs of the decision tree are the same as the states for RL. After the decision tree is well trained, the decision tree algorithm is able to select the key inputs as the parameters at the nodes to decide the window opening area and the cooling setpoint at each time step.

In specific, given the input vector X_t at time step t and corresponding action label y_t , the decision tree recursively partitions the input space such that the samples with the same action are grouped [46]. Let λ_m with N_m samples represent the data at node m . For each candidate split θ , partition the data into $\lambda_m^{left}(\theta)$ and $\lambda_m^{right}(\theta)$ subsets

$$\lambda_m^{left}(\theta) = \{(x, y) | x < t_m\} \quad (14)$$

$$\lambda_m^{right}(\theta) = \lambda_m \setminus \lambda_m^{left}(\theta) \quad (15)$$

where t_m is the threshold of the candidate split θ .

The quality of a candidate split of node m is then computed using an impurity function $H()$:

$$G(\lambda_m, \theta) = \frac{N_m^{left}}{N_m} H(\lambda_m^{left}(\theta)) + \frac{N_m^{right}}{N_m} H(\lambda_m^{right}(\theta)) \quad (16)$$

$$H(\lambda_m) = \sum_k p_{mk}(1 - p_{mk}) \quad (17)$$

where p_{mk} is the proportion of class k observations in the node m .

To make the decision tree have the best accuracy in representing the prediction of RL, select the parameters that minimise the impurity

$$\theta^* = \operatorname{argmin}_\theta G(\lambda_m, \theta) \quad (18)$$

After the optimal θ^* is calculated, the knowledge of the RL is successfully extracted. The above calculation for the optimal tree structure is conducted using scikit-learn [47].

2.4. Testbed for the mixed-mode ventilation

Figure 2 shows a plan view of the testbed, an MMV office designed for eight occupants. The ventilation mode of the testbed office is the change-over MMV, which means the office switches between operating in air conditioning mode (AC mode) and NV mode. Specifically, when the office operates in NV mode, the window is open, and the AC is off; when the office operates in AC mode, the window is closed, and the AC is operating. The external wall with an operable window is built with 200mm concrete with insulation of Glass fiber and gypsum board. This wall is facing west with one operable window. The operable window is 2.8m in width and 1.2m in height. The other three external walls of the testbed are built with 2×16 mm gypsum plasterboard on both sides with 100mm steel stud infilled with rock wool insulation. The HVAC system of the testbed office is a hybrid system that combines a typical VAV system with two ceiling fans. The ceiling fans are able to provide an occupied zone with an air velocity of 0.3–1.1m/s. To provide the best indoor thermal comfort, the ceiling fans are operated at the level that makes the occupied zone with PMV close to zero according to the indoor temperature. The simulation period is an entire year using the hourly weather data of Singapore. The time step is 30 min for the minimum HVAC and window operation interval. The control strategy decides the window opening area and the cooling setpoint at each time step. The HVAC system is off

during the non-operation hour. The HVAC systems are sized to meet the cooling load in Singapore. We built a virtual testbed to simulate the operation of mixed-mode ventilation in this testbed using EnergyPlus (version 9.4) [48] and the AirFlow Network module [49] is utilized to calculate the outdoor air flow rate when the window is open. Both rule-based control and RL control are simulated for comparison. To confirm the reliability of the AirFlow Network module in natural ventilation simulation, we compared the air change measurement results (SF6 concentration decay method) and the simulation results with a window opening percentage of 50%. As shown in Figure 3, the simulation results are close to the measurement results, indicating the reliability of the AirFlow network.

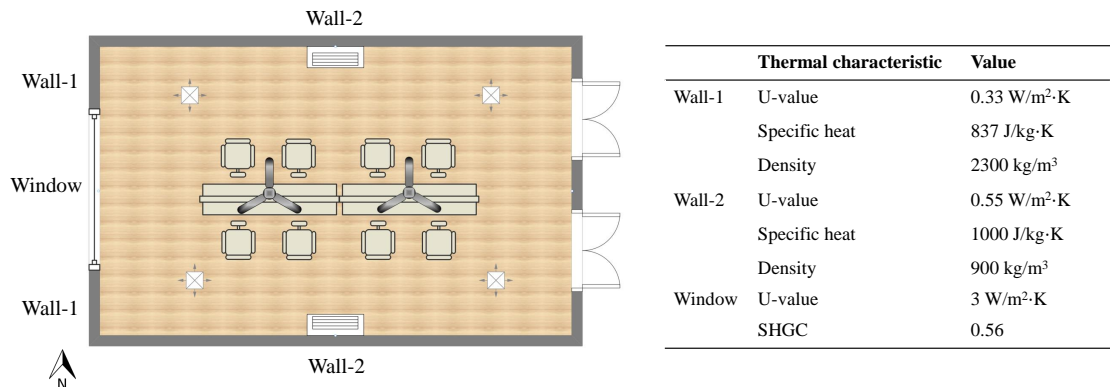


Figure 2: The plan of the testbed for the MMV office

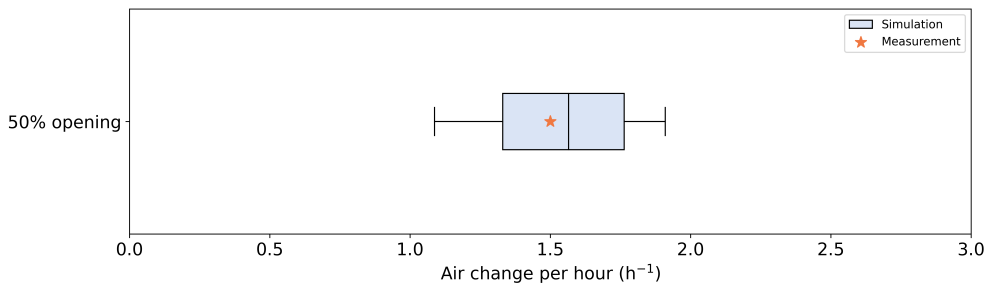


Figure 3: Comparison of air change per hour between measurement and simulation results. (The simulation results are based on the whole year simulation with RL-3 strategy)

The proposed RL control strategy and the baseline control strategy are applied to the testbed office under tropical climate, which is the climate in Singapore. The outdoor temperature and relative humidity of Singapore in 2018 are shown in Figure 4. The daily temperature range has a minimum usually not falling below 22-25 °C during the night and a maximum not rising above 31-33°C during the day. Relative humidity varies from around 90% in the morning just before sunrise, and falls to around 60% - 70% in the mid-afternoon on days.

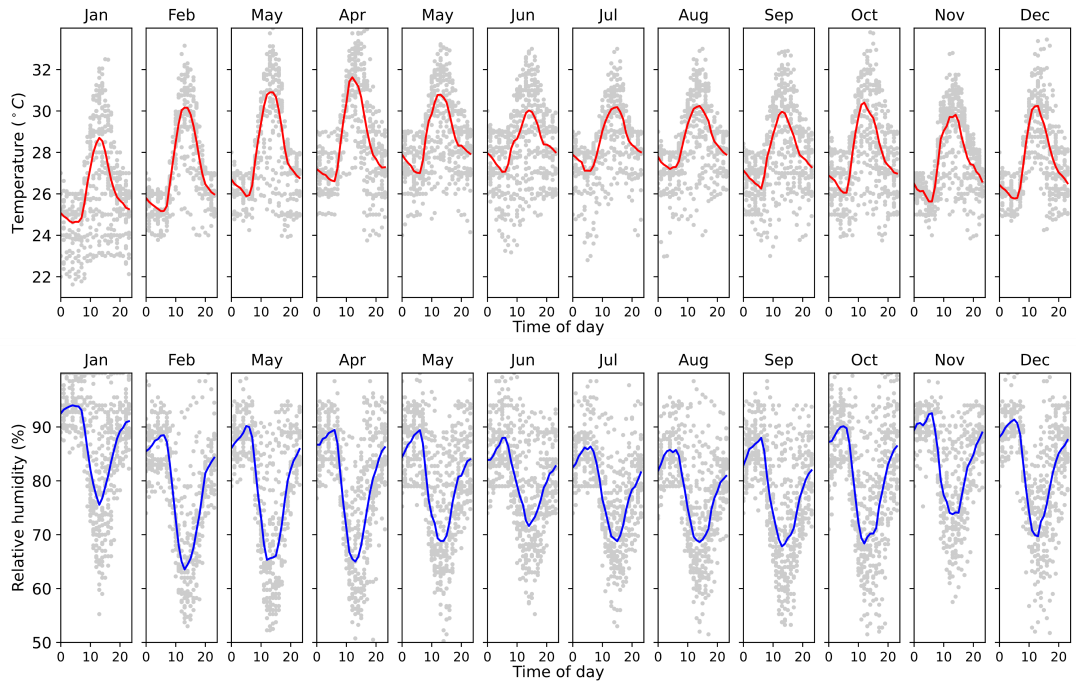


Figure 4: Hourly outdoor dry-bulb temperature (top plot) and relative humidity (bottom plot) in Singapore split by month for the year 2018.

3. Results

3.1. Performance comparison

For evaluation, we compared the three RL strategies with two baseline rule-based controls typically used for mixed-mode operations (Table 2). Table 4 presents the annual indoor thermal environment, air quality and the corresponding cooling energy consumption under different control strategies. Under the baseline-29 strategy, there is 40% of time in NV. The corresponding annually-averaged cooling energy is $299 \text{ kWh}/m^2\text{yr}$. and the percentage of comfort time is 84%. As the threshold of the opening window increases to 30°C , the percentage of time in NV increases to 58% and the annually-averaged cooling energy decreases to $228 \text{ kWh}/m^2\text{yr}$. However, the percentage of comfort time decreases from 84% to 58%. By comparing the baseline-29 and baseline-30, it can be seen that the outdoor temperature of 29°C is the upper bound of the threshold for the baseline strategy. A higher threshold will lead to an unsatisfactory indoor thermal environment. Therefore, we use baseline-29 as the baseline strategy for the following analysis.

Figure 5 shows the cumulative cooling energy consumption for the virtual testbed each month. Under the baseline-29 strategy, the monthly cumulative cooling energy consumption ranges from 600 kWh to 1500 kWh, while it ranges from 300 kWh to 600 kWh across all three RL strategies (Table 2). Under the RL-1 strategy, the percentage of comfort time is still maintained above 80%. The RL-1 strategy is able to significantly decrease the cooling energy while maintaining a comfortable indoor environment by increasing the time in NV at the suitable time. As shown in

Table 4

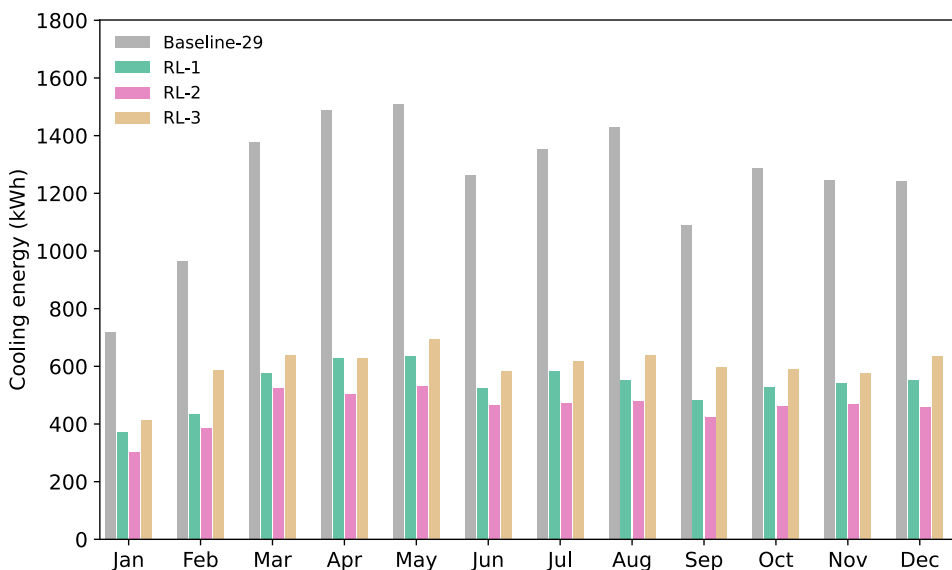
Comparison of the cooling energy, time in NV and the corresponding indoor environment under different control strategies for MMV. (Note that the comfort time means the percentage of time satisfying adaptive thermal comfort requirement during NV operation)

Strategy ¹	Cooling energy (kWh/m ² yr.)	Time in NV ² (%)	Mean ACH during NV time (h ⁻¹)	Comfort time (%)	CO ₂ ¹ (ppm)
Baseline-29	299	40	6.6	84	749
Baseline-30	228	58	6.5	58	692
RL-1	128	76	0.28	80	1244
RL-2	109	75	0.26	80	1367
RL-3	144	58	1.51	81	862

¹ Results presented are for operating hours (8 a.m. - 7 p.m.).

² Percentage of operating hours when the building is operating in NV.

Table 4, the annual percentage of time in NV increases to 76% by applying the RL-1 control strategy for the MMV control, and the annually-averaged cooling energy decreases by 57% to 128 kWh/m²yr.. The reason for the significant energy saving is that the RL-1 strategy switch between AC and NV mode to take advantage of the thermal mass for precooling. By doing this, the RL-1 strategy significantly increases the time in NV while maintaining a similar indoor thermal comfort time. Given that the cooling energy during NV time is zero, the increase of time in NV leads to a significant improvement in energy saving.

**Figure 5:** The cumulative cooling energy consumption under different strategies in each month

Compared with RL-1, RL-2 further decreases cooling energy by 15% to 109 kWh/m²yr. while maintaining a similar comfort time. For the RL-2 strategy, the cooling setpoint is added as a control variable of the RL strategy. Due to this, the cooling setpoint increases at some suitable time to save cooling energy without significant impacts on the

time in NV. This indicates that the proposed RL strategy can minimize the cooling energy by optimizing the window opening schedule and the cooling setpoint during AC mode. However, since indoor air quality is not considered as a constraint during the training period of the RL-1 and RL-2 strategies, the indoor CO₂ concentration is higher than 1000 ppm under the RL-1 and RL-2 strategies.

Compared with the RL-2 strategy, the cooling energy increases by 32%, which is 144 kWh/m² yr.. This is because the CO₂ concentration is considered as an additional constraint for the RL-3 strategy. Due to this constraint, the minimal window opening percentage increases to 50%. More outdoor air is introduced to maintain good IAQ, leading to increased heat gain from the outdoor air. By doing this, the mean CO₂ concentration during operation hour is 862 ppm, which is lower than the guideline of 1000 ppm. Under this strategy, the percentage of time in NV is 58%, which is slightly lower than that under RL-1 and RL-2 strategies. This is because the opening area of the window under RL-3 is generally larger than that under RL-1 and RL-2, which limits the NV availability for some time when the outdoor environment is hot. However, compared with the baseline strategy, the RL-3 strategy still achieves a significant energy saving rate of 52%. This shows that the proposed RL strategy is able to save cooling energy while maintaining good occupant thermal comfort and indoor air quality.

Figure 6 shows the Pareto Front of the energy consumption and adaptive comfort time for the three RL strategies. Among these strategies, the RL-3 strategy consumes the most cooling energy while the RL-2 consumes the least when the percentage of adaptive thermal comfort times are similar. Also, it can be seen that for the three RL strategies, the cooling energy consumption increases as the percentage of adaptive thermal comfort time increases. This is because there are fewer hours that would meet these requirements in NV as we increase thermal comfort requirements, making the cooling energy increase. Compared with baseline-29 which consumes 299 kWh/m² a. for cooling and has 84% of time within the adaptive thermal comfort zone, the RL-3 strategy performs better than the baseline in both energy saving and comfort time. With 95% of time in the adaptive comfort zone, the cooling energy is 194 kWh/m² a. under the RL-3 strategy, which is 35% lower than the cooling energy under the baseline strategy.

The relationships between the daily cooling energy and outdoor temperatures under different strategies are shown in Figure 7. Under the baseline-29 strategy, the cooling energy in NV increases significantly as outdoor air temperature increases. The daily cooling energy is about 60 kWh when the outdoor temperature is above 30 °C. Under RL strategies, the growth rate of cooling energy with outdoor temperature is not as large as that under the baseline-29 strategy. When the outdoor temperature is above 30 °C, the cooling energy ranges from 10 kWh to 30 kWh. The daily cooling energy under the RL-3 strategy is around 5 kWh higher than that under the RL-2 strategy.

3.2. Insights to RL using XAI

Figure 8 shows the SHAP values for the action of operating in the AC mode of the trained RL-3 agent. The SHAP values present the importance of four features on the decision of the RL agent. The positive SHAP values indicate a

positive influence on the decision while the negative values indicate a negative influence. It can be seen that indoor temperature and outdoor temperature are the most two important features in deciding the operation of the AC mode with higher absolute SHAP values, while the outdoor RH and solar radiation have a relatively small influence on the decision of the RL. Moreover, regarding the influence of indoor temperature, the SHAP values show positive when the

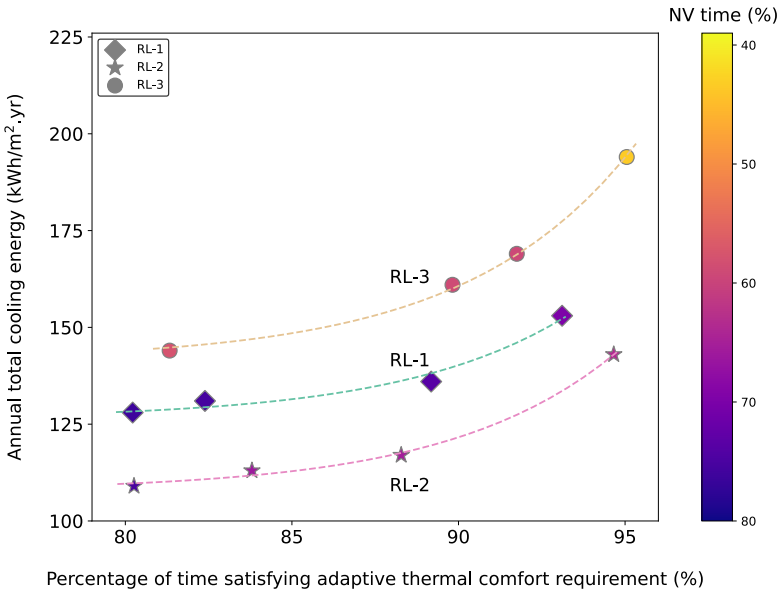


Figure 6: The Pareto Front of the energy consumption and the percentage of time satisfying adaptive comfort requirement for the three RL strategies

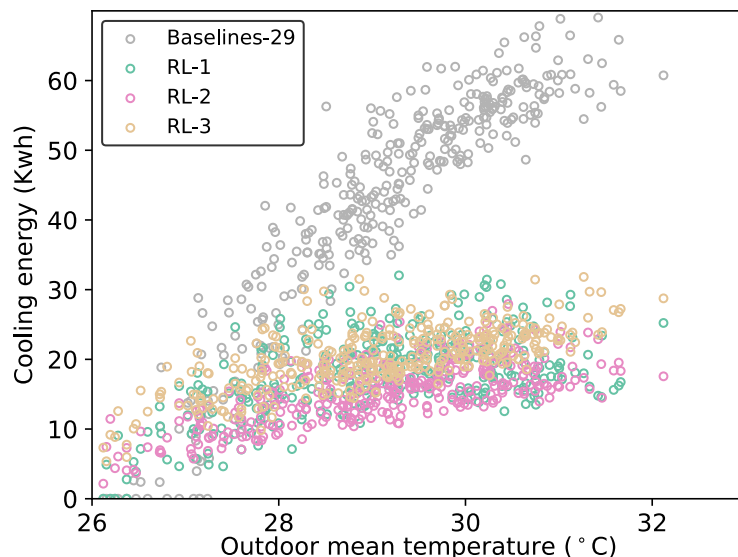


Figure 7: The scatter plot of daily cooling energy and the corresponding averaged outdoor air temperature under different strategies

indoor temperature is high. This indicates the RL agent tends to run in AC mode when the indoor temperature is high, which is reasonable since we need to maintain a suitable indoor thermal comfort. Regarding the impact of outdoor temperature, the positive SHAP values come with relatively low outdoor temperature. The reason for this is that the RL agent tends to run the AC mode in advance to take advantage of the thermal mass when the outdoor temperature is relatively low, which helps to increase the cooling efficiency. By presenting the SHAP values of the RL agent, it provides insights for us to understand the process of the RL strategy, engendering appropriate trust for the RL strategy.

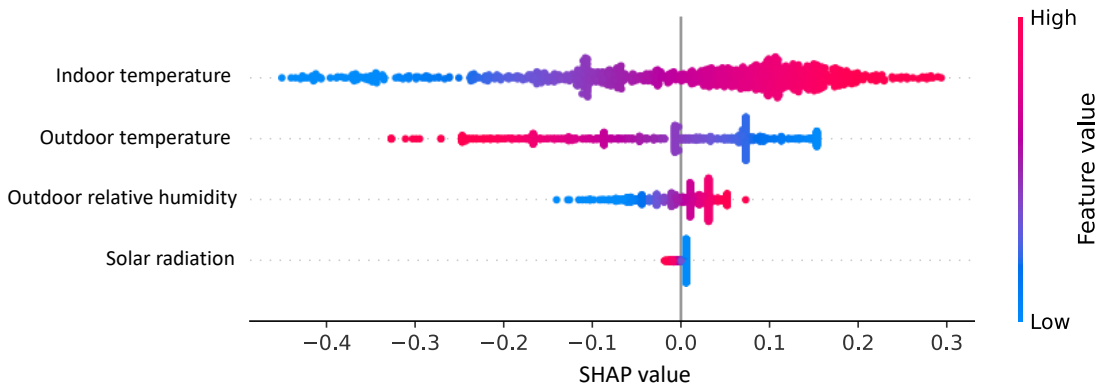


Figure 8: The SHAP values of the trained RL-3 agent

In order to better understand the control principles of the RL-3, we used the decision tree algorithm to extract the control rules from the control schedule of the RL-3. As shown in Figure 9, the decision tree selected indoor and outdoor temperature as the important features at the nodes, which is consistent with the results of the SHAP analysis above. Compared to the states of the RL, the solar radiation and outdoor relative humidity were not included as the parameters at the nodes. The reason for not including the solar radiation is that the simulation building is well shaded in this study, and the solar radiation does not have a significant impact on cooling energy. For outdoor relative humidity, this is because the outdoor RH is relatively stable in Singapore. The decision tree does not take it as an informative feature to consider as a parameter at the tree nodes. The cooling setpoint and the window opening area are controlled by the following four rules according to the indoor and outdoor environment at the last time step:

- Rule 1: the window are fully open at t if outdoor air temperature is lower than 27°C at $t - 1$;
- Rule 2: the window open with 50% at t if indoor is lower than 27°C but outdoor is higher than 27°C at $t - 1$.
- Rule 3: the window is closed and the cooling setpoint is 25°C at t if outdoor temperature is between $[27^{\circ}\text{C}, 29^{\circ}\text{C}]$ and indoor temperature is higher than 27°C at $t - 1$.
- Rule 4: the window is closed and the cooling setpoint is 27°C at t if outdoor temperature is higher than 29°C and indoor temperature is higher than 27°C at $t - 1$.

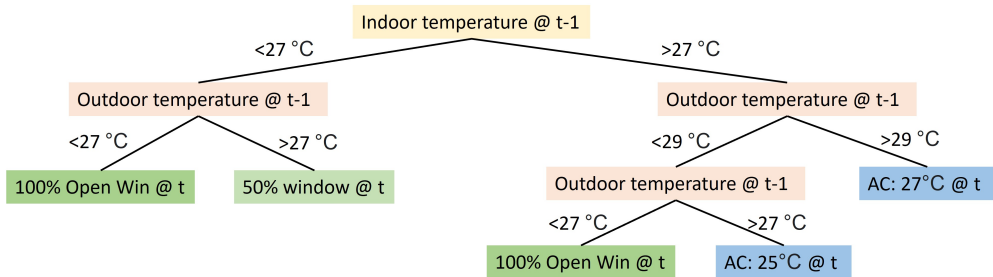


Figure 9: The decision tree for the window opening and the cooling setpoint extracted from RL-3 with 80% of adaptive thermal comfort time

We could gain further insights into what RL-3 considers desirable for effective MMV through the extracted rules. When the outdoor air temperature is lower than 27 °C at the last time step (Rule 1), the window is fully opened to take advantage of the desirable outdoor environment. When the outdoor air temperature is higher than 27 °C and indoor air temperature is lower than 27 °C at the last time step, NV is acceptable but the window opening area should not be too large to keep the indoor environment within the adaptive thermal comfort zone. Therefore, the window opening area is 50% in this situation. When the outdoor air temperature is between [27°C, 29°C] and indoor air temperature is higher than 27°C at $t - 1$, the indoor environment is close to the upper bound of the adaptive thermal comfort zone. In this situation, the AC is operating to maintain a comfortable indoor environment. The cooling setpoint is set at 25 °C to make NV available for the next time step. In other words, the precooling strategy is conducted to increase the time in NV and save cooling energy. When the outdoor air temperature is higher than 29 °C and the indoor temperature is higher than 27 °C at $t - 1$ (Rule 4), the precooling cannot provide additional time in NV. Therefore, the cooling setpoint is set at 27 °C for this situation to save cooling energy.

What stands out from the generalized rules is that the cooling setpoint is different between Rule 3 and Rule 4. When the outdoor temperature is between [27°C, 29°C] and the indoor temperature is higher than 27°C, Rule 3 takes advantage of the indoor thermal mass by turning down the setpoint to increase the time in NV. To better understand this process, Figure 10 (a) shows the wall inside surface temperature profile for a typical day. When the AC is operating for 30 min with the cooling setpoint at 25 °C, and the outdoor temperature is between [27°C, 29°C] (Rule 3), the wall inside surface temperature decreases by around 0.3 °C. During the AC mode, as shown in 10 (b), the convection heat transfer rate between the inside surface and indoor air is about 500 W. Some cooling energy is stored in the internal thermal mass by the convection heat transfer. After Rule 3 is executed, the room temperature is usually lower than 27 °C. According to the extracted rules, the window opens at 50% for 1 hour. During the 1 hour in NV mode, the wall inside surface temperature increases about 0.8 °C. Part of the stored cooling energy is used to remove the radiant heat gain from internal sources and windows. Meanwhile, with the outdoor air rate of 75L/s (window opening area of 50%), the indoor air temperature will not go beyond the thermal comfort limit when the indoor/outdoor temperature

difference is about 1 °C. The cooling storage in thermal mass is sufficient to remove radiant heat gain from indoor sources and windows. This indicates that the cooling setpoint of 25 °C can take advantage of indoor thermal mass to increase NV time when the outdoor temperature is between [27°C, 29°C]. In comparison, if the outdoor temperature is higher than 29 °C, the air temperature difference between indoor and outdoor increases to around 3 °C. Under this situation, the heat gains from outdoor air increase three times if opening the window at 50% for 1 hour. Under this condition, the internal thermal mass cannot provide enough cooling to maintain a comfortable indoor environment for 1 hour in NV. Since the cooling setpoint of 25 °C cannot provide additional NV time under this condition, it is increased to 27 °C to save energy, as Rule 4 does.

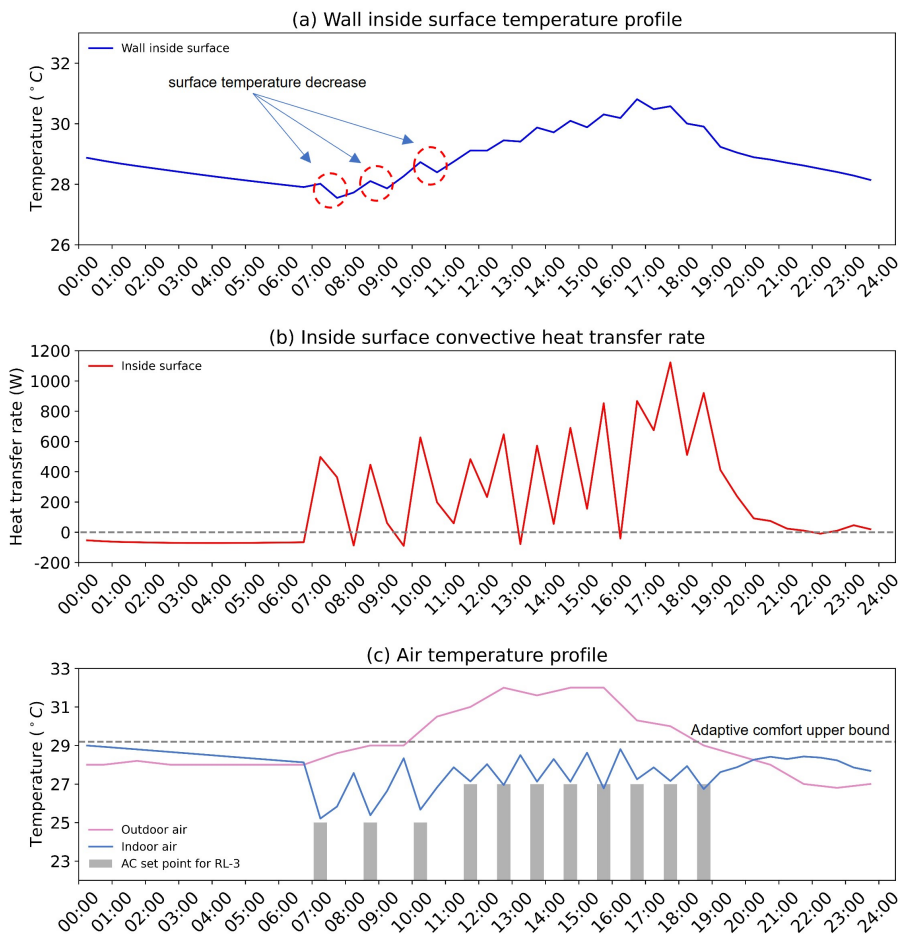


Figure 10: The wall inside surface temperature, convective heat transfer rate, outdoor air and indoor air in a typical day under RL-3

3.3. Performance of extracted rules

To investigate the performance of the extracted rules, we compared the cooling energy consumption and the corresponding percentage of adaptive thermal comfort time under RL-3 and extracted rules. As shown in Table 5,

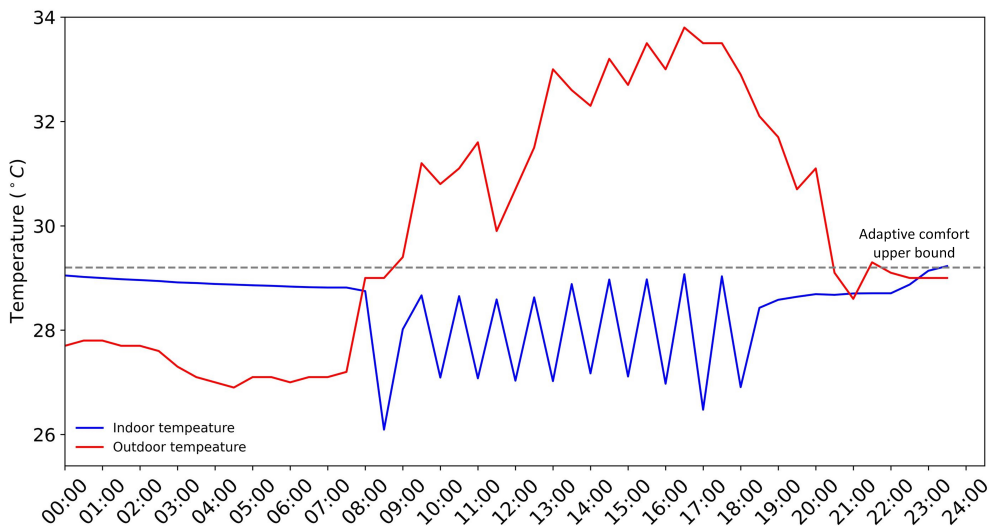
Table 5

Comparison of indoor environment parameters under the RL-3 control strategy and extracted-rules for MMV control

	RL-3	Extracted-rules	Difference
Cooling energy ($\text{kWh}/\text{m}^2\text{a.}$)	144	133	-8%
Comfort time (%)	81	79	-3%
Time in NV (%)	58	62	6%
CO_2 concentration (ppm)	862	869	1%

the cooling energy is $133 \text{ kWh}/\text{m}^2\text{yr}$. with 79% of time within the adaptive thermal comfort zone under the extracted rules. In comparison, the cooling energy is $144 \text{ kWh}/\text{m}^2\text{yr}$. with 81% of time within the adaptive thermal comfort zone under the RL-3 strategy. The comfort time was reduced by 3% by using extracted rules instead of the RL strategy as the control strategy. There is no significant difference between the control performance of extracted rules and the RL-3 strategy. It can be concluded that the decision tree is able to extract reliable and implementable rules from the RL strategies, which are also understandable to humans.

The extracted rules are further applied to the actual testbed. As shown in Figure 11, the testbed switches between operating in AC mode and NV mode during the operation hour. Compared with the baseline strategy, the time in NV increased by 50% under this rule. Moreover, the indoor temperature was maintained below the adaptive thermal comfort limit throughout the whole day, showing a good thermal environment during MMV.

**Figure 11:** The indoor temperature profile for an actual testbed under extracted rules

3.4. Typical days analysis

Figure 12 compares the window opening schedule and the indoor temperature under baseline-29 and RL-1 strategy for a typical day. On this day, the outdoor temperature keeps above 27°C for the whole day. From 1:00 p.m. - 4:00

p.m., the outdoor air temperature reaches its peak at about 32 °C. Under the baselines-29 strategy, the window is fully open in the early morning and late evening, and the AC is operating from 9:00 a.m. - 6:30 p.m. with a setpoint of 24 °C. The total time in NV during operation hours is 2.5h. With this window opening schedule, the indoor temperature first increases to its daily peak value of 29.5 °C at 9:00 a.m. and then maintains at 24 °C until 6:30 p.m. After that, the indoor temperature increases to 27 °C again as the window is open from 6:30 p.m. - 7:00 p.m. In comparison, the RL-1 strategy switches the NV mode and AC mode during the operation hour. In the morning, the window opens for 1.5h after the AC operates for 0.5h. In the afternoon, the window opens for 1 hour after the AC operates for 0.5h. Generally, the AC operates when the indoor temperature is close to the upper bound of the adaptive thermal comfort zone; the window is open when the indoor environment is cool to save energy. Moreover, the RL-1 strategy opens the window with a small opening area of 25%. By doing this, the heat gain from the outdoor air is reduced, and the time in NV is hence maximized. For this typical day, the time in NV under the RL-1 strategy is 6h longer than that under the baseline-29 strategy.

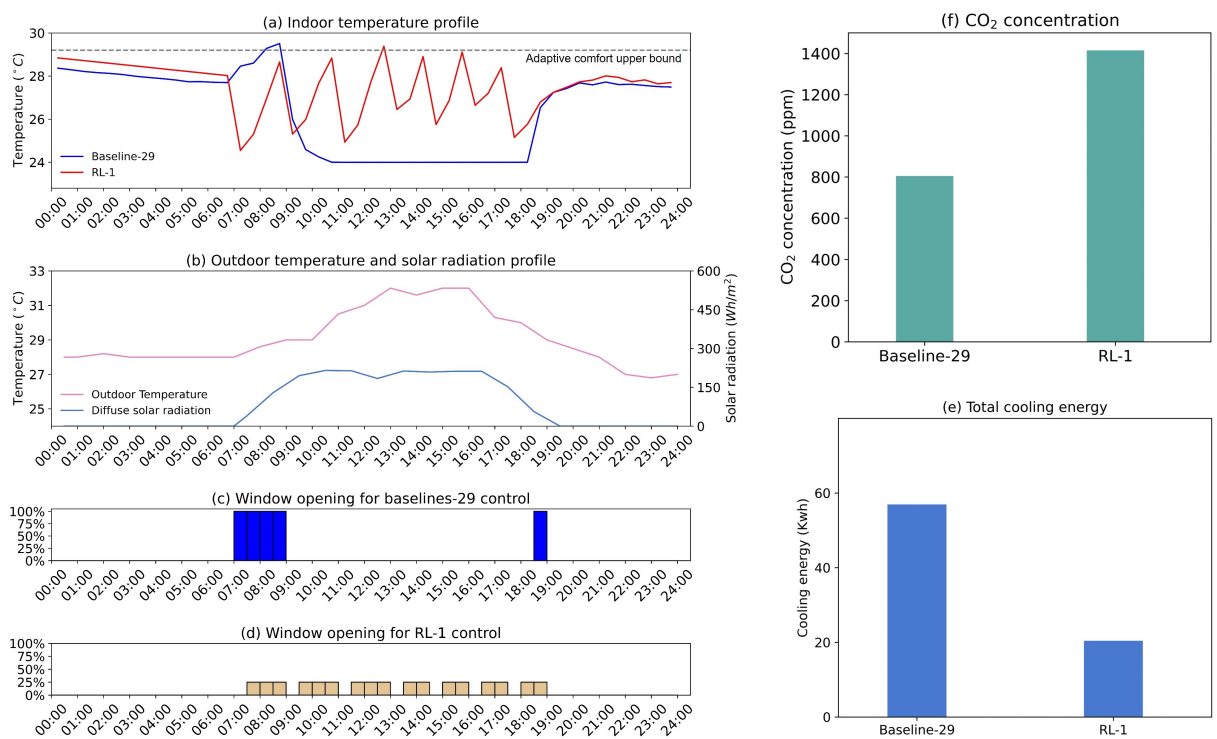


Figure 12: Comparison of indoor temperature, window opening schedule, indoor CO₂ and cooling energy by baseline and RL-1 strategy for a typical day

Figure 13 shows the window opening and the cooling setpoint schedule under the RL-2 strategy. Compared with the RL-1 strategy, the RL-2 strategy adds the cooling setpoint as an additional control variable. As shown in 13(a), the RL-2 strategy raises the cooling setpoint to 25 °C in the morning and the late afternoon. During this period, raising

the cooling setpoint does not decrease the time in NV. Moreover, the cooling energy further decreases a little due to the increase of the cooling setpoint. Compared with the RL-1 strategy, the cooling energy is reduced by 25% under the RL-2 strategy for this day.

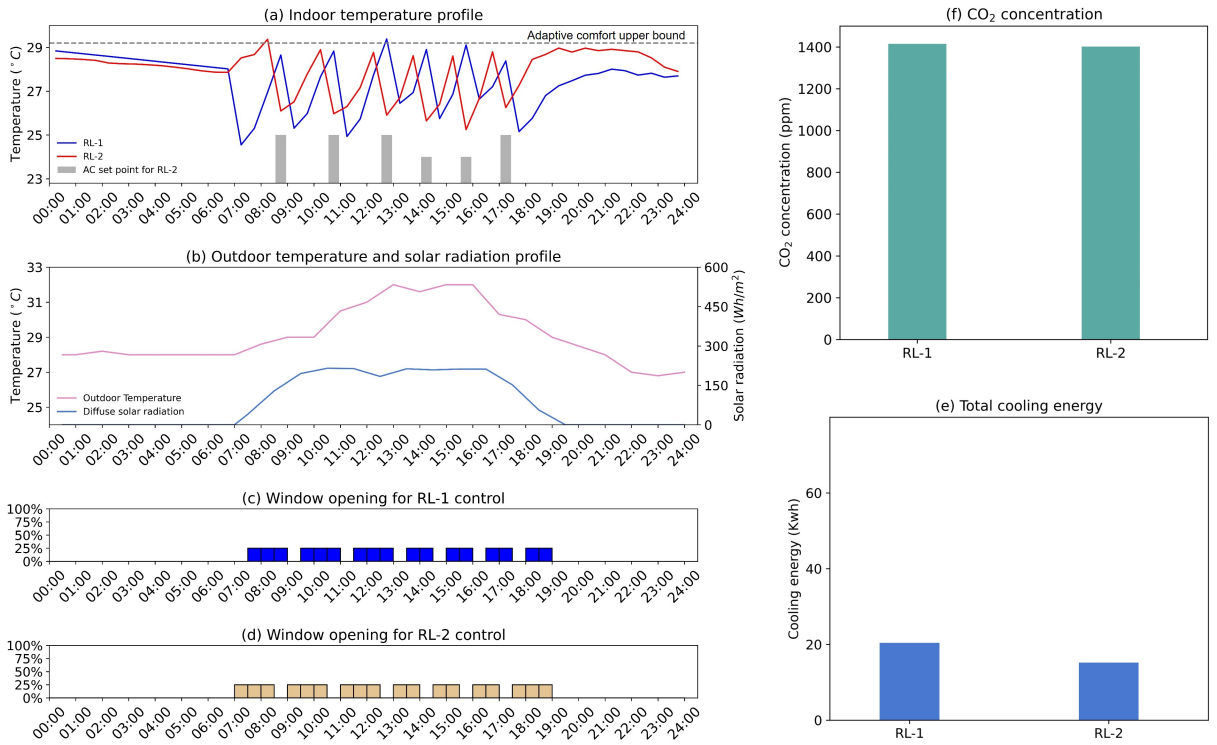


Figure 13: Comparison of indoor temperature, window opening schedule, indoor CO₂ and cooling energy by RL-1 and RL-2 strategy for a typical day

Figure 14 shows the window opening and the cooling setpoint schedule under the RL-3 strategy. Compared with the RL-1 and RL-2 strategies, the RL-3 strategy is trained with an additional constraint of indoor CO₂ concentration lower than 1000 ppm. Due to this constraint, as shown in Figure 14, the window is open with 50% to provide about 75 L/s outdoor air for maintaining good IAQ. Regarding the cooling setpoint, it is also set at 25 °C in the morning. This is consistent with explanations provided by the XAI framework that the RL agent tends to run the AC mode in advance to take advantage of the thermal mass when the outdoor temperature is relatively low. However, the RL-3 strategy sets the cooling setpoint at 27 °C in the afternoon and switches the AC and NV mode every half hour. This is different from the schedule of the RL-2 strategy that sets the cooling setpoint at 24 °C. The reason for this difference is that the minimal window opening is 50% after adding indoor CO₂ concentration as an additional constraint, and the heat gain from outdoor air therewith increases as the window opening area increases. With a ventilation rate of 75L/s, the thermal capacity cannot provide enough cooling energy during this time. The larger outdoor fresh air rate makes

the indoor thermal capacity insufficient to keep the NV mode for 1 hour. Therefore, the RL-3 strategy has to switch the NV and AC modes every half hour. Meanwhile, the RL-3 strategy also increases the cooling setpoint to 27 °C to minimize the cooling energy.

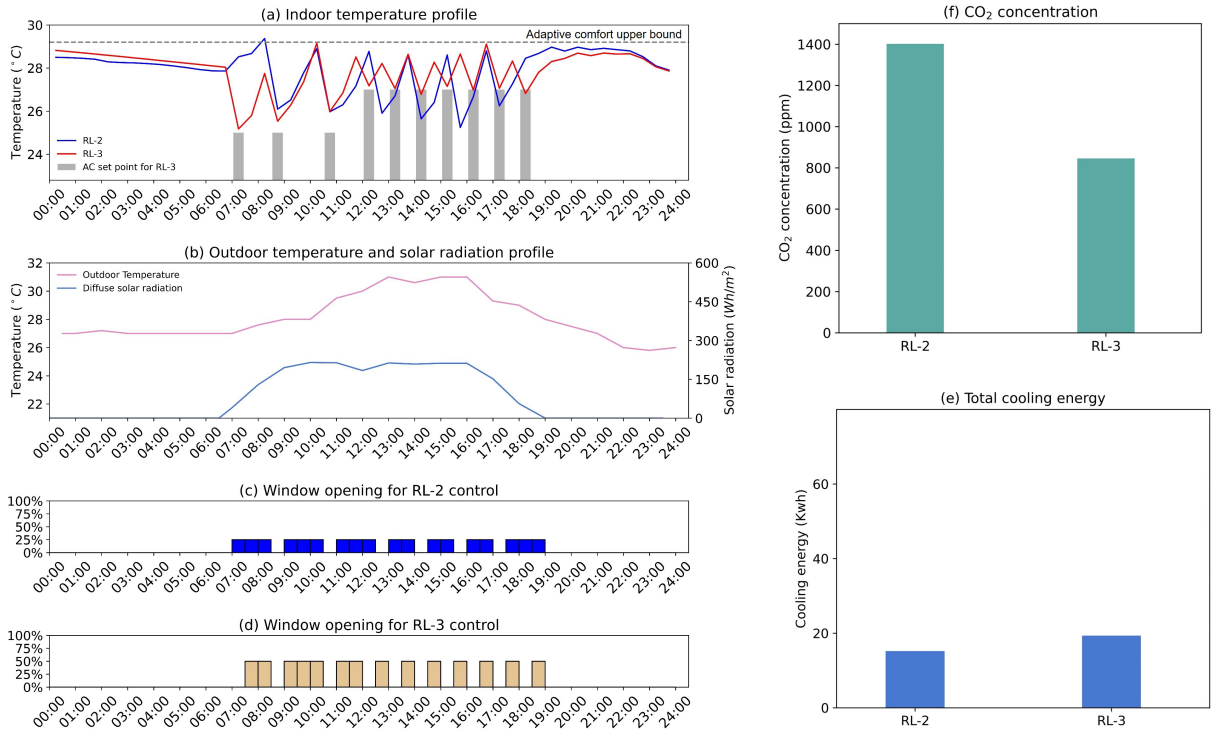


Figure 14: Comparison of indoor temperature, window opening schedule, indoor CO₂ and cooling energy by RL-2 and RL-3 strategy for a typical day

4. Discussion

4.1. RL to maximize energy saving for MMV

The RL algorithm is applied to control the MMV for the office building. The control variables of the RL algorithm in this study include the window opening area and the cooling setpoint, which is different from previous studies that control binary window status(open/close) for MMV [22, 23]. In this way, the proposed RL algorithm decreases the cooling energy for MMV buildings significantly by optimizing the ventilation mode and the related control variables. Specifically, the RL can maximize the NV time by flexibly switching AC/NV mode while maintaining good indoor thermal comfort. Moreover, by integrating window opening as a control variable, the window is open at the optimal opening area to reduce the heat gain from the introduction of outdoor air when the outdoor environment is hot, and meanwhile to make sure enough outdoor air for good IAQ. Regarding the cooling setpoint, the higher cooling setpoint is able to reduce cooling energy significantly while the lower setpoint might be able to provide more NV potential

for the next time step. Therefore, the cooling setpoint is also taken into consideration for the MMV control. To our knowledge, this is the first study that integrates these two control variables for the control of MMV using RL.

4.2. XAI for insights to MMV control

Although the trained RL has shown good performance for control of MMV, it is not transparent and cannot provide general understanding to humans, which makes it lack reliability. One effective way to solve this problem is to find the surrogate model that globally approximates the predictions of the black-box model [50]. In this study, we use Kernel SHAP to provide insights into the decision-making process of the RL agent, prompting the trust and understanding of the RL strategy. Furthermore, a white-box surrogate model, decision tree, is used to learn the prediction of RL. By doing this, the critical control rules of the RL can be extracted. Furthermore, the extracted rules are combined with the knowledge of building physics to interpret the control principle of the RL strategy. Using XAI, this study also identified that the RL algorithm was taking advantage of the internal thermal mass to increase cooling efficiency, pointing to the importance of passive design for achieving effective MMV. According to the simulation results of the case study, the extracted rules achieved similar control performance as the RL strategy, showing the effectiveness of the XAI approaches. Moreover, due to the transparency and interpretability of the decision tree, the extracted XAI rules can be double-checked by engineering to confirm their reliability and provide new insights regarding the control of MMV.

4.3. Feasibility of the extracted rules

Since the control agent of the RL is a fully connected network, it involves complicated calculations and lacks maintainability. After XAI extracts the key control rules, the decision tree provides straightforward control logic for MMV buildings. Compared to the RL strategy, the extracted rules are easier to be implemented in the building management system. Moreover, it is easier for engineers to understand the control logic.

Currently, we use an MMV building in the tropics as a case study. The XAI approach provides reliable control rules for the testbed office. After it is applied to more different buildings, the high-level knowledge about the control of the MMV buildings can be generalized by combining knowledge from building science and machine learning. With this high-level knowledge, other engineers can easily design the MMV control strategies for their buildings without spending much time training the RL algorithms.

4.4. Directions for further development

In this study, we investigate the energy-saving potential of MMV for the office in the tropic. It is worthy of applying the RL strategy for buildings in other climate zones since studies have confirmed that the energy-saving potential of MMV is impacted by climate significantly [13]. Furthermore, by interpreting the optimal RL control strategy, the XAI is promising to bridge the gap between building science and the RL strategy, especially for problems involving complex interactions between sub-systems. Future studies may focus on using XAI to explore the transparent, explainable and

reliable high-level knowledge for MMV control, which is helpful for engineers to design MMV control strategies for different buildings without the need to train the AI algorithm for each building. In another aspect, it is interesting to implement these advanced control strategies for real MMV buildings and compare the performance of the data-driven control strategy and MPC strategy [51], as well as the corresponding IAQ under different strategies [52]. Last but not least, the rules extracted by XAI approach does not require predictive information to make decision. It is interesting to further study whether MPC is necessary for MMV control and what can we further benefit from integrating predictive information into MMV control.

5. Conclusions

This study applies RL to optimize the control of change-over MMV. By applying the RL strategy to a virtual testbed office in the tropic, it is shown that the RL is able to identify relationships that can further reduce cooling energy use while maintaining occupant thermal comfort. Furthermore, XAI is applied to bridge the gap between building science and the RL strategy, which prompts building scientists toward new insights into MMV control in the tropics. The main conclusions are as follows:

- RL is able to improve the energy performance of MMV buildings by 1) flexibly switching between NV and air-conditioning based on outdoor and indoor conditions, and 2) optimizing the window opening area and the cooling setpoint.
- RL can achieve a 52% reduction in cooling energy while maintaining good thermal comfort and indoor air-quality performance compared to the existing baselines.
- Energy savings were comparable between the rules extracted by the XAI approach and the original RL. According to the knowledge extracted by XAI, the RL algorithm was taking advantage of the internal thermal mass to increase cooling efficiency.

Acknowledgements

This research is supported by the National Research Foundation, Singapore, and Ministry of National Development, Singapore under its Cities of Tomorrow R&D Programme (CoT Award COT-V4-2020-5). Any opinions, findings and conclusions or recommendations expressed in this material are those of the author(s) and do not reflect the views of National Research Foundation, Singapore and Ministry of National Development, Singapore.

References

- [1] Agency, I.E.. Global status report for buildings and construction 2019. IEA Paris, France; 2019.,

- [2] Hou, D., Lin, C.C., Katal, A., Wang, L.L.. Dynamic forecast of cooling load and energy saving potential based on ensemble kalman filter for an institutional high-rise building with hybrid ventilation. In: Building Simulation; vol. 13. Springer; 2020, p. 1259–1268.
- [3] Kim, J., de Dear, R.. Is mixed-mode ventilation a comfortable low-energy solution? a literature review. *Building and Environment* 2021;205:108215.
- [4] Salcido, J.C., Raheem, A.A., Issa, R.R.. From simulation to monitoring: Evaluating the potential of mixed-mode ventilation (mmv) systems for integrating natural ventilation in office buildings through a comprehensive literature review. *Energy and Buildings* 2016;127:1008–1018.
- [5] Ezzeldin, S., Rees, S.J.. The potential for office buildings with mixed-mode ventilation and low energy cooling systems in arid climates. *Energy and Buildings* 2013;65:368–381.
- [6] Wang, H., Chen, Q.. A semi-empirical model for studying the impact of thermal mass and cost-return analysis on mixed-mode ventilation in office buildings. *Energy and Buildings* 2013;67:267–274.
- [7] Daaboul, J., Ghali, K., Ghaddar, N.. Mixed-mode ventilation and air conditioning as alternative for energy savings: a case study in beirut current and future climate. *Energy Efficiency* 2018;11(1):13–30.
- [8] Chen, Y., Tong, Z., Malkawi, A.. Investigating natural ventilation potentials across the globe: Regional and climatic variations. *Building and Environment* 2017;122:386–396.
- [9] Mihara, K., Chen, S., Hasama, T., Tan, C.L., Lee, J.K.W., Wong, N.H.. Environmental satisfaction, mood and cognitive performance in semi-outdoor space in the tropics. *Building and Environment* 2022;:109051.
- [10] Ono, E., Mihara, K., Lam, K.P., Chong, A.. The effects of a mismatch between thermal comfort modeling and hvac controls from an occupancy perspective. *Building and Environment* 2022;:109255.
- [11] Mihara, K., Sekhar, C., Takemasa, Y., Lasternas, B., Tham, K.W.. Thermal comfort and energy performance of a dedicated outdoor air system with ceiling fans in hot and humid climate. *Energy and Buildings* 2019;203:109448.
- [12] Miller, D., Raftery, P., Nakajima, M., Salo, S., Graham, L.T., Peffer, T., et al. Cooling energy savings and occupant feedback in a two year retrofit evaluation of 99 automated ceiling fans staged with air conditioning. *Energy and Buildings* 2021;251:111319.
- [13] Bamdad, K., Matour, S., Izadyar, N., Omrani, S.. Impact of climate change on energy saving potentials of natural ventilation and ceiling fans in mixed-mode buildings. *Building and Environment* 2022;209:108662.
- [14] Brager, G.. Mixed-mode cooling. 2006;.

- [15] Breesch, H., Bossaer, A., Janssens, A.. Passive cooling in a low-energy office building. *Solar Energy* 2005;79(6):682–696.
- [16] Eftekhari, M., Marjanovic, L.. Application of fuzzy control in naturally ventilated buildings for summer conditions. *Energy and buildings* 2003;35(7):645–655.
- [17] Wang, L., Greenberg, S.. Window operation and impacts on building energy consumption. *Energy and Buildings* 2015;92:313–321.
- [18] Fiorentini, M., Serale, G., Kokogiannakis, G., Capozzoli, A., Cooper, P.. Development and evaluation of a comfort-oriented control strategy for thermal management of mixed-mode ventilated buildings. *Energy and Buildings* 2019;202:109347.
- [19] Zhan, S., Chong, A.. Data requirements and performance evaluation of model predictive control in buildings: A modeling perspective. *Renewable and Sustainable Energy Reviews* 2021;:110835.
- [20] Chen, Y., Tong, Z., Zheng, Y., Samuelson, H., Norford, L.. Transfer learning with deep neural networks for model predictive control of hvac and natural ventilation in smart buildings. *Journal of Cleaner Production* 2020;254:119866.
- [21] Zhan, S., Lei, Y., Jin, Y., Yan, D., Chong, A.. Impact of occupant related data on identification and model predictive control for buildings. *Applied Energy* 2022;323:119580.
- [22] May-Ostendorp, P., Henze, G.P., Corbin, C.D., Rajagopalan, B., Felsmann, C.. Model-predictive control of mixed-mode buildings with rule extraction. *Building and Environment* 2011;46(2):428–437.
- [23] Hu, J., Karava, P.. A state-space modeling approach and multi-level optimization algorithm for predictive control of multi-zone buildings with mixed-mode cooling. *Building and Environment* 2014;80:259–273.
- [24] Hu, J., Karava, P.. Model predictive control strategies for buildings with mixed-mode cooling. *Building and Environment* 2014;71:233–244.
- [25] Spindler, H.C., Norford, L.K.. Naturally ventilated and mixed-mode buildings—part ii: Optimal control. *Building and Environment* 2009;44(4):750–761.
- [26] Zhang, Z., Chong, A., Pan, Y., Zhang, C., Lam, K.P.. Whole building energy model for hvac optimal control: A practical framework based on deep reinforcement learning. *Energy and Buildings* 2019;199:472–490.
- [27] Wang, Z., Hong, T.. Reinforcement learning for building controls: The opportunities and challenges. *Applied Energy* 2020;269:115036.
- [28] Lei, Y., Zhan, S., Ono, E., Peng, Y., Zhang, Z., Hasama, T., et al. A practical deep reinforcement learning framework for multivariate occupant-centric control in buildings. *Applied Energy* 2022;324:119742.

- [29] Wang, H., Ding, Z., Tang, R., Chen, Y., Fan, C., Wang, J.. A machine learning-based control strategy for improved performance of hvac systems in providing large capacity of frequency regulation service. *Applied Energy* 2022;326:119962.
- [30] Zhang, Q., Lin, M., Yang, L.T., Chen, Z., Li, P.. Energy-efficient scheduling for real-time systems based on deep q-learning model. *IEEE transactions on sustainable computing* 2017;4(1):132–141.
- [31] Chen, Y., Norford, L.K., Samuelson, H.W., Malkawi, A.. Optimal control of hvac and window systems for natural ventilation through reinforcement learning. *Energy and Buildings* 2018;169:195–205.
- [32] Luo, M., Cao, B., Damiens, J., Lin, B., Zhu, Y.. Evaluating thermal comfort in mixed-mode buildings: A field study in a subtropical climate. *Building and environment* 2015;88:46–54.
- [33] Kim, J., Tartarini, F., Parkinson, T., Cooper, P., De Dear, R.. Thermal comfort in a mixed-mode building: Are occupants more adaptive? *Energy and Buildings* 2019;203:109436.
- [34] Srinivasan, S., Arjunan, P., Jin, B., Sangiovanni-Vincentelli, A.L., Sultan, Z., Poolla, K.. Explainable ai for chiller fault-detection systems: gaining human trust. *Computer* 2021;54(10):60–68.
- [35] Arrieta, A.B., Díaz-Rodríguez, N., Del Ser, J., Bennetot, A., Tabik, S., Barbado, A., et al. Explainable artificial intelligence (xai): Concepts, taxonomies, opportunities and challenges toward responsible ai. *Information fusion* 2020;58:82–115.
- [36] Lundberg, S.M., Lee, S.I.. A unified approach to interpreting model predictions. *Advances in neural information processing systems* 2017;30.
- [37] Sundararajan, M., Taly, A., Yan, Q.. Axiomatic attribution for deep networks. In: International conference on machine learning. PMLR; 2017, p. 3319–3328.
- [38] Heo, J., Lee, H.B., Kim, S., Lee, J., Kim, K.J., Yang, E., et al. Uncertainty-aware attention for reliable interpretation and prediction. *Advances in neural information processing systems* 2018;31.
- [39] Alvarez Melis, D., Jaakkola, T.. Towards robust interpretability with self-explaining neural networks. *Advances in neural information processing systems* 2018;31.
- [40] Sheh, R., Monteath, I.. Introspectively assessing failures through explainable artificial intelligence. In: IROS Workshop on Introspective Methods for Reliable Autonomy. iliad-project. eu Vancouver, Canada; 2017, p. 40–47.
- [41] Sturmfels, P., Lundberg, S., Lee, S.I.. Visualizing the impact of feature attribution baselines. *Distill* 2020;5(1):e22.
- [42] Peng, Y., Lei, Y., Tekler, Z.D., Antanuri, N., Lau, S.K., Chong, A.. Hybrid system controls of natural ventilation and hvac in mixed-mode buildings: A comprehensive review. *Energy and Buildings* 2022;112509.

- [43] <https://pytorch.org/docs/stable/generated/torch.nn.SmoothL1Loss.html>. Feb. 18, 2022.
- [44] <https://github.com/slundberg/shap>. Feb. 18, 2022.
- [45] Adadi, A., Berrada, M.. Peeking inside the black-box: a survey on explainable artificial intelligence (xai). *IEEE access* 2018;6:52138–52160.
- [46] <https://scikit-learn.org/stable/modules/tree.html#tree>. Feb. 18, 2022.
- [47] Pedregosa, F., Varoquaux, G., Gramfort, A., Michel, V., Thirion, B., Grisel, O., et al. Scikit-learn: Machine learning in Python. *Journal of Machine Learning Research* 2011;12:2825–2830.
- [48] <https://energyplus.net/>. Feb. 18, 2022.
- [49] Gu, L.. Airflow network modeling in energyplus. In: Building Simulation; vol. 10. 2007,.
- [50] Došilović, F.K., Brčić, M., Hlupić, N.. Explainable artificial intelligence: A survey. In: 2018 41st International convention on information and communication technology, electronics and microelectronics (MIPRO). IEEE; 2018, p. 0210–0215.
- [51] Jia, L., Liu, J., Chong, A., Dai, X.. Deep learning and physics-based modeling for the optimization of ice-based thermal energy systems in cooling plants. *Applied Energy* 2022;322:119443.
- [52] Liu, S., Koupriyanov, M., Paskaruk, D., Fediuk, G., Chen, Q.. Investigation of airborne particle exposure in an office with mixing and displacement ventilation. *Sustainable Cities and Society* 2022;79:103718.